Sibutramine, a serotonin-norepinephrine reuptake inhibitor, causes fibrosis in rats

Hester Magdalena Oberholzer[a]; Ciska van der Schoor[a]; Megan Jean Bester[a]

[a]Department of Anatomy, Faculty of Health Sciences, University of Pretoria, Pretoria, South Africa

Corresponding author:

HM Oberholzer

Department of Anatomy

Faculty of Health Sciences

University of Pretoria

Private Bag x323

ARCADIA

0007

SOUTH AFRICA.

Email: nanette.oberholzer@up.ac.za

Tel: (+27)12 319 2533 / Fax: (+27)12 319 2240

Abstract

Sibutramine hydrochloride monohydrate is a weight loss agent indicated for the treatment of obesity. Although it has been banned from most markets, studies are still relevant as it is often a hidden ingredient in herbal and over the counter slimming products. Sibutramine induces liver fibrosis with steatosis in female Sprague-Dawley rats fed a high-energy diet without significant weight gain. In this study, using the same animal model, the effect of Sibutramine on lung morphology was investigated using histological evaluation of the terminal bronchiole and transmission electron microscopy evaluation of the respiratory tissue. From these results Sibutramine was found to induce lung fibrosis in Sprague-Dawley rats as increased collagen synthesis, mast cell accumulation and aggregates of Bronchus Associated Lymphoid Tissue (BALT) in the terminal bronchiole as well as increased collagen deposition in the respiratory tissue was seen.

Key words: Sibutramine, fibrosis, mast cells, iBALT, collagen

1. Introduction

Sibutramine hydrochloride monohydrate is a monoamine reuptake inhibitor. Its therapeutic effects are produced mainly by the inhibition of norepinephrine (NE) and serotonin (5-hydroxytryptamine, 5-HT) reuptake at neuronal synapse sites in the Central Nervous System (CNS). This inhibition causes an increase in the synaptic concentration of these substances and consequently an increase in the feeling of satiety and energy expenditure and a resultant decrease in food intake (Lechin *et al.,* 2006; Eroglu *et al*., 2009; Sansbury BE and Hill BG, 2014). After absorption, Sibutramine is metabolized by the hepatic Cytochrome P450 enzymes, forming the pharmacologically active metabolites, M1 and M2, which are responsible for the resultant hypophagic effect and subsequent weight-loss (Hwang IC *et al.,* 2014; Luque and Rey 2002; Padwal and Majumdar 2007). Despite Sibutramine's initial success as weight reducing agent, it was later banned from most markets following a series of reported adverse events including death. However, it is still available via the internet and many herbal products have been shown to contain far higher concentrations of this product than that which was prescribed.

Most of the human body's 5-HT is located in the enterochromaffin cells within the gastrointestinal tract, where it is responsible for regulating intestinal movements. It is also stored in platelets contributing to haemostasis and blood clotting. In certain cell types, 5-HT has been identified as a growth factor and has been shown to increase the proliferation of fibroblasts and consequent collagen synthesis that can lead to fibrosis (Fabre *et al.*, 2008). These findings have further been substantiated by Dees *et al*., (2011) who linked elevated 5-HT levels to vascular disease and tissue fibrosis due to its ability to stimulate extracellular matrix production in both sclerotic and healthy fibroblasts. There are two 5-HT receptor subtypes that have been identified to play an important role in the lungs specifically. These are receptors 5-HT_{2A} and 5-HT_{2B} (Fabre *et al.,* 2008). Following Sibutramine administration, the reuptake of 5-HT is blocked resulting in the activation of serotonergic receptors, and ultimately prolonged tissue exposure. It can therefore be hypothesised that prolonged exposure to raised 5-HT levels will cause increased risk for lung associated fibrosis as a result of 5-HT mediated activation of fibrogenesis.

Diet induced obese animals have become the standard for studies investigating obesity and its co-morbid complications. In such a model, using Sprague-Dawley rats, Jackson *et al*., (1997) described the hypophagic effects of Sibutramine and identified the key adrenoreceptors and serotonergic receptors involved in its pharmacological mechanism. In a study to determine the safety of Sibutramine it was observed that, following Sibutramine

administration, ultrastructural changes in morphology associated with fibrosis in liver tissue in Sprague-Dawley rats fed a high energy diet that did not result in weight gain, could be observed by Oberholzer *et al.* (2013). In this study the effects Sibutramine on lung morphology was further investigated by using light- and transmission electron microscopy.

2. Materials and methods:

2.1. *Implementing the Spraque-Dawley rat model*

Sprague-Dawley rats fed a high energy diet were implemented in this study. Ethical clearance was obtained from the University of Pretoria Animal Use and Care committee (ethical clearance number: h015-11). Thirty female, sexually mature Sprague-Dawley rats, each of average weight (200-250g) were used in this study and were maintained at the University of Pretoria Biomedical Research Centre (UPBRC). The animals were housed conventionally in cages complying with the sizes laid down in the SANS 10386:2008 recommendations. A room temperature of 22°C (±2); relative humidity of 50% (±20) and a 12hr light/dark cycle was maintained. Enrichment was provided according to standard procedures at the UPBRC. This experiment was conducted over a period of 88 days.

The animals were randomly divided into three groups [NC (Normal chow), HED (high energy diet) and HED-S (high energy diet plus Sibutramine administration)] with ten animals per group as indicated in Table 1.

Table 1. Experimental design indicating the diet, treatment and treatment periods of the animals in the three experimental groups

Group	Diet	Treatment	Days 0-59	Days 60-88
NC	Normal chow	None	Normal chow	Normal chow
HED	High energy diet	None	High energy diet	High energy diet
HED-S	High energy diet	Sibutramine	High energy diet	High energy diet plus Sibutramine

All animals were fed on the normal diet [Epol mice cubes; a division of Rainbow farms (Pty) Ltd, Westville, Johannesburg, South Africa] for the first four days. This served as an acclimatization period. For statistical purposes, day 0 was taken on the first day the animals in the HED groups received the high energy diet. Animals in the NC group remained on the normal chow diet for the duration of the study. Animals in the HED group were on the HED

from day 5 until day of termination (days 0 – 88). Animals in the HED-S group were on the HED from day 5 until day of termination, but were treated with Sibutramine for the last 28 days before termination. This allowed time for the animals to gain weight on the HED before treatment with the weight loss agent commenced. Four weeks is also the standard time period for toxicology studies. During the last 28 days, animals in the NC and HED groups were not treated with the solvent of Sibutramine as it was dissolved in sterile water and water was provided *ad libitum* to all animals.

2.2. High energy diet (HED)

The HED diet consisted of 12% corn oil, 43% condensed milk and 45% Epol pellets. The nutritional value was estimated to be 4.4Kcal/g with 13% protein, 18% fat and 69% carbohydrate content. The normal chow diet was replaced with the HE diet and was available to the animals *ad libitum*.

2.3. Sibutramine administration

Animals in the HED-S group were treated with 1.32mg/kg b. wt. dose of Sibutramine hydrochloride monohydrate (BIOCOM biotech; Clubview, South Africa) dissolved in sterile water for 28 days. This dosage concentration was extrapolated from an equivalent human dose (i.e. 15mg/day) using the formula for dose translation based on body surface area (BSA) as described by Reagan-Shaw *et al*. (2007). Sibutramine was administered to each animal in this group every morning (08h00) via oral gavage. This route of administration ensured that all animals within an experimental group received exact, equal concentrations of the test compound and was done by proper handling methods by trained individuals to avoid any unnecessary discomfort to the animals.

2.4. Tissue for light microscopy

On the final day of experimentation (day 28) rats were terminated via Isoflurane overdose. Tissue samples were collected via dissection and lung samples were fixed in 2% formaldehyde in phosphate buffered saline for 12-24 hours and were then dehydrated in an ethanol series, cleared with xylene and embedded in paraffin wax. Sections of 4-6µm were stained with picrosirius red and luna stain respectively and images viewed at 10x and 40x magnification with a Nikon Trans Optiphod transmitted light microscope (Nikon Instech Co., Kanagawa, Japan).

2.5. Picrosirius red staining

For the evaluation of the formation of different collagen fibers, the slides were stained with picrosirius red. The slides were de-waxed following standard protocols and then stained with Haematoxylin for 8 minutes after which they were washed for 10 minutes in running water. The slides were then counterstained with picrosirius red (1mg/ml in saturated picric acid solution) for one hour, after which they were washed in two changes of acidified water and dehydrated three times in 100% ethanol. The slides were then examined using both polarised and normal light.

2.6. Luna stain

The luna stain was used to indicate the presence of mast cells in the tissue. Slides were de-waxed and rehydrated with 95% ethanol. Afterwards they were stained with aldehyde fuchin for 30 minutes, rinsed 3 times in 95% ethanol and then stained with haematoxylin for 10 minutes. Following haematoxylin staining, the slides were rinsed with running tap water for 10 minutes followed by a single rinse in 95% ethanol. Methyl orange stain was applied for 10 minutes after which slides were then dehydrated and mounted.

2.7. Tissue for transmission electron microscopy

Lung samples were fixed in 2.5% glutaraldehyde/formaldehyde for 1 hour, rinsed three times in 0.075M sodium potassium phosphate buffer (pH=7.4) for 15 minutes before being placed in secondary fixative, 1% osmium tetraoxide solution, for 1 hour. Following fixation, the samples were rinsed again as described above. This was followed by dehydration in 30%, 50%, 70%, 90% and three changes of 100% ethanol. Samples were then embedded in resin and ultra-thin sections (80-100nm), cut with a diamond knife using an ultramicrotome, were contrasted with uranyl acetate for 5 minutes followed by 2 minutes of contrasting with lead citrate, after which samples were allowed to dry and examined with the JEOL transmission electron microscope (TEM) (JEM 2100F).

3. Results

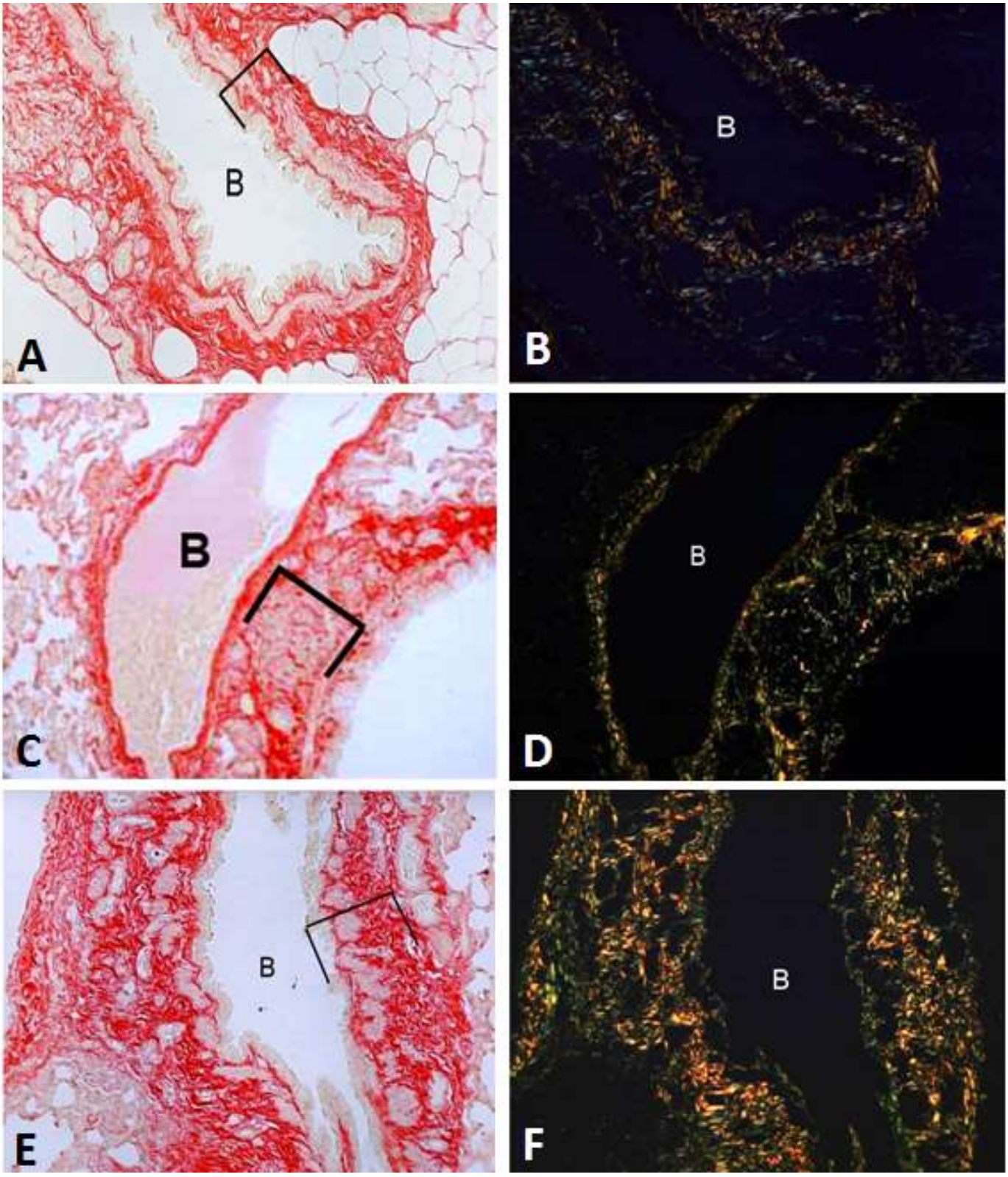

Figure 1. Light microscopy micrographs of lung tissue of animals in the NC group (A and B); HED group (C and D) and HED-S group (E and F) stained with picrosirius red. Without polarised light (A, C and E) and polarised light (B, D and F). B (Bronchus)

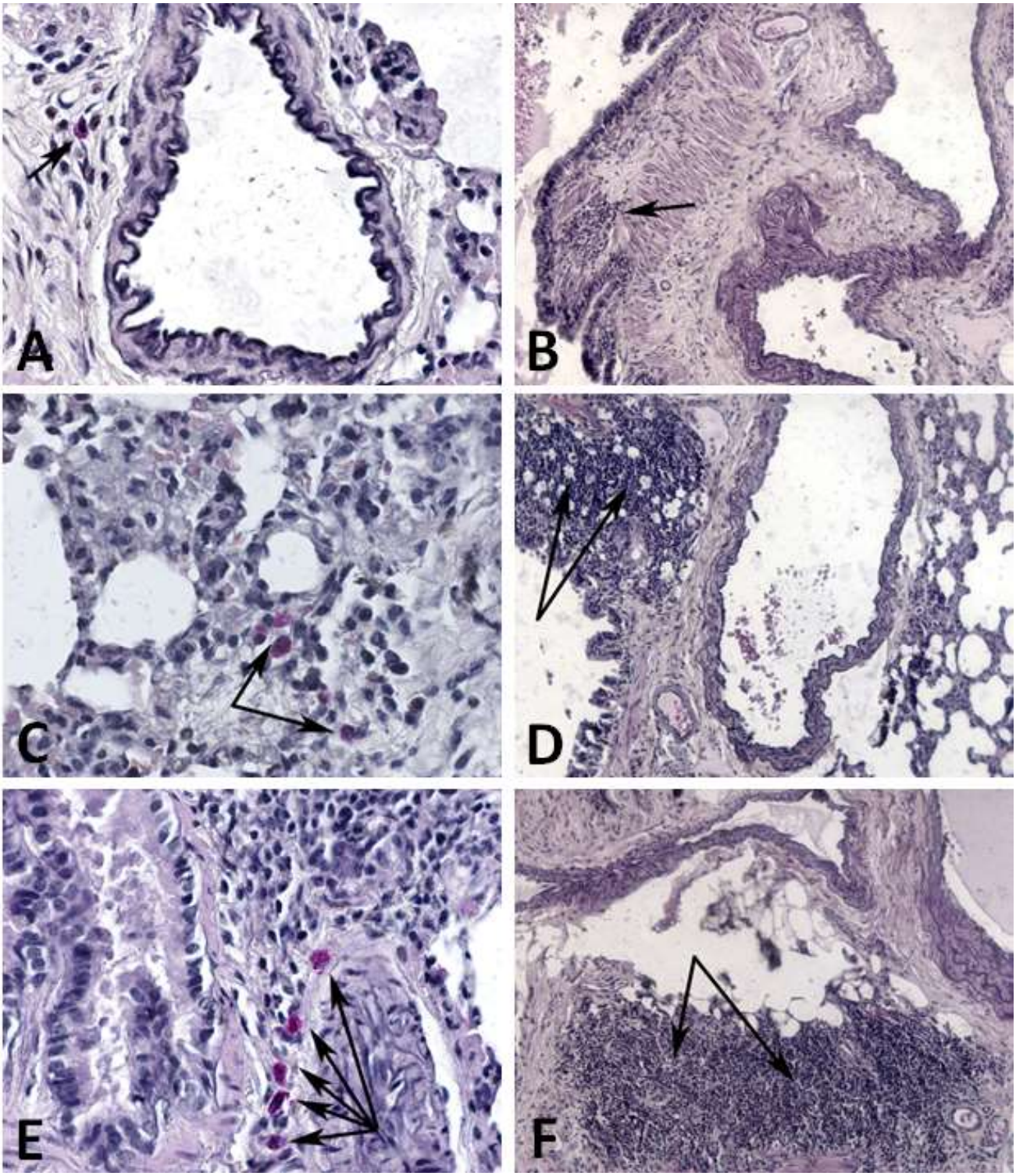

Figure 2. Light microscopy micrographs of lung tissue of animals in the NC group (A and D); HED group (B and E) and HED-S group (C and F) stained with Luna stain. Black arrows in A, B and C indicate the presence of mast cells, and those in D, E and F indicate the accumulation of lymphoid tissue

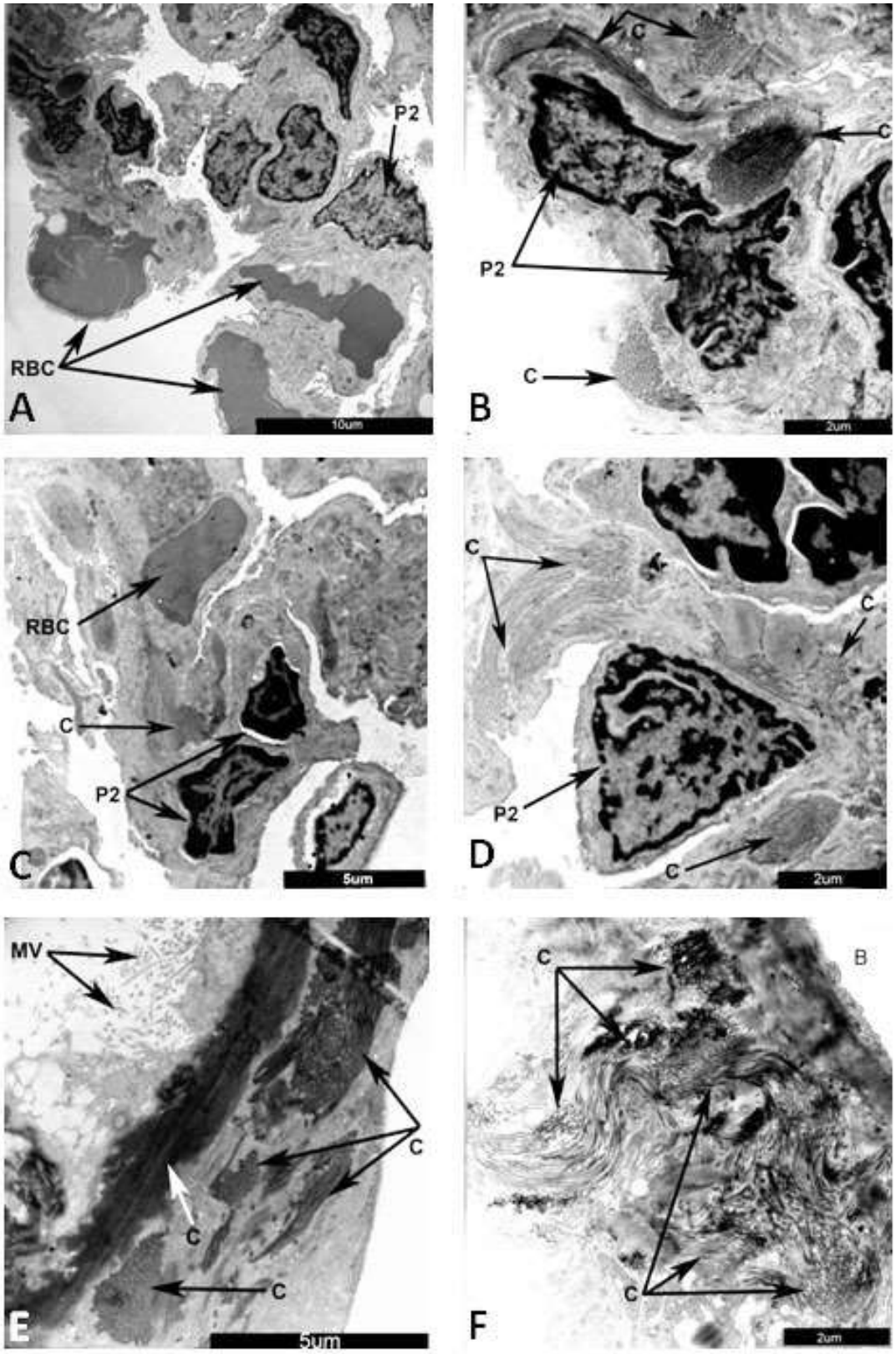

.

Figure 3. TEM micrographs of lung tissue of animals in the NC group (A and B); HED group (C and D) and HED-S group (E and F). Collagen bundles (arrows). RBC (Red blood cells); P2 (pneumocytes type II); MV (microvilli); C (collagen); B (Bronchus).

The distribution of collagen in lung tissue of NC, HED and HED-S treated rats was evaluated. Figure 1 shows the terminal bronchiole with the associated connective tissue stained with picrosirius red. Images taken with and without polarised light are shown indicating thicker collagen fibres (stained yellow) as well as thinner fibres (stained green). Figure 1 A and B are representative of lung tissue of the control animals (NC group), with the well-defined terminal bronchial wall with its characteristically folded respiratory epithelium and regularly arranged oval bundles of smooth muscle clearly visible. The connective tissue surrounding the terminal bronchial consists of light yellow staining fibres. Figure 1 C and D are from animals in the HED group. A thickened area adjacent to the bronchial wall can be seen indicated by the black block in Figure 1 C and a similar area is visible in Figure 1 D, as shown with polarized light. Compared to the controls the intensity of the stain is increased and within the indicated area, finer green staining fibres are present. Figures 1 E and F show lung tissue from animals on the HED, together with Sibutramine treatment for 28 days. In Figure 1 E, increased fibrotic areas are shown surrounding the terminal bronchiole and with polarized light, as seen in Figure 1 E, the stain is more intense with thicker, compactly arranged, yellow staining fibres which infringes or penetrates into the smooth muscle layers.

Figure 2 A-F are light micrographs of lung tissue from animals in the three experimental groups stained with the luna stain to show the presence of mast cells in the lung periphery (A, B and C) and the accumulation of lymphoid tissue [(BALT), (D, E and F)]. Only a few mast cells could be seen in the control samples, indicated by the black arrow in Figure 2 A. In the HED and HED-S groups more mast cells could be identified, when compared to the control group, with grouping of mast cells seen in some areas. This is indicated in Figure 2 B and C and could not be seen in the control animals. Figure 2 D, E and F show the presence of lymphoid tissue or accumulation of lymphocytes in the control, HED and HED-S groups respectively. In the control group, very few areas of lymphoid cells could be found compared to the accumulation of lymphoid cells seen in the HED group (Figure 2 E) and the comparably large mass of cells found in the HED-S group (Figure 2 F).

Increased collagen deposition was also observed using transmission electron microscopy in the distal respiratory region at the site of gaseous exchange. Figures 3 A-F are TEM micrographs of the lung alveolar region showing the presence of increased collagen deposition, indicated with black arrows. Figure 3 A and B show normal alveolar ultrastructural arrangement showing the presence of the alveolar space, capillaries, and pneumocytes (Figure 3A) and at a higher magnification collagen associated with the interalveolar space can be seen (Figure 3B). Figures 3 C and D are representative of

animals in the HED group where a slight increase in collagenous bundles could be seen compared to the control group. However, in Figure 3 E and F, which represents animals in the HED-S group, the accumulation of collagen bundles (indicated by the black arrows) as well as thickened masses of collagen fibres (white arrow) associated with the interalveolar space, identified by the presence of microvilli on the luminal surface and the presence of membrane bound spherical bodies, were seen.

4. Discussion

Sibutramine has been shown to cause liver fibrosis in rats fed a HE diet without weight gain (Oberholzer *et al*., 2013). This was based on morphological analysis of liver tissue which showed an observable increase in collagen deposition and lipid accumulation within hepatic stellate cells, which have been shown to increase extracellular matrix production following liver injury (Moreira, 2007).

In this study the structural morphology of the lungs of NC, HED and HED-S treated rats was evaluated with specific focus on the terminal bronchiole and the respiratory tissue using light- and transmission electron microscopy respectively.

5-HT is believed to play a vital role in the lung and of the 14 5-HT receptors identified the two subtypes involved in the lungs have been shown to be 5-HT_{2A} and 5-HT_{2B} (Loric *et al.,* 1995; Marcos *et al*., 2004). Receptor 5-HT_{2A}, is fibroblast associated and is selectively increased in inducible pulmonary fibrosis (IPF) whereas 5-HT_{2B} is mainly found in lung epithelium. Fabre and colleagues have shown that the 5-HT pathway act on many different cells in the lungs, including pneumocytes type II, epithelial bronchial cells, pleural mesothelial cells and also lung fibroblasts (Fabre *et al*., 2008). Known effects of 5-HT in the respiratory system include pulmonary arterial constriction, bronchoconstriction and stimulation of hyperplastic and hypertrophic alterations in smooth muscle cells and myofibroblasts. The latter causes changes in lung architecture resulting in increased pulmonary vascular resistance and/or lung fibrosis (Mann and Oakley, 2013). Pulmonary fibrosis is characterised by the deposition of excessive amounts of the extracellular matrix protein, collagen, as well as increases in cells associated with collagen synthesis and inflammation (Sime and O'Reilly 2001; Phan, 2002; Blaauboer *et al*., 2014).

Sibutramine is a monoamine reuptake inhibitor that results in increased extracellular levels of 5-HT. A 5 day treatment of Sprague-Dawley rats with 10mg/kg Sibutramine resulted in a

significant increase in the plasma concentration of serotonin and is associated with fibrosis of the liver, heart and lung (Mann and Oakley, 2013). Fibrosis of the lung can be associated with many chronic diseases but can also be drug-induced. However, little is known about the effect Sibutramine may have on the lungs of an individual.

Fibroblasts are present throughout the lamina propria of the conducting pathway of the lungs. The lamina propria consists mainly of a network of capillaries as well as a meshwork of reticular fibers continuous with the basement membrane. Ultrastucturally it has been shown that this region is populated with fibroblasts that can interact with adjacent epithelial cells and are involved with local inflammatory and reparative processes (Fraser, 2005). In respiratory tissue a basement membrane is also associated with type I and II pneumocytes and is locally fused with the basement membrane underlying the endothelial cells of the alveolar capillaries. The pro-proliferative and pro-fibrotic properties of 5-HT (Fabre *et al*., 2008) may account for the increased fibrotic tissue present in the interalveolar space of rats fed a HED-S diet, essentially resulting in increased deposition of collagen.

Intratracheal instillation of bleomycin is a widely used rodent experimental model for drug induced lung fibrosis (Latta *et al*., 2015). Izbicki *et al*., (2002) reported that following 2 weeks exposure, mice lung tissue had multifocal or diffuse changes that included thickened alveolar septa, inter-alveolar fibrosis with myofibroblasts within the lumen, occasional foci of dense fibrosis, increased alveolar macrophages and focal dilation of respiratory bronchioles and alveolar ducts. Likewise, Sibutramine was found to cause increased inter-alveolar fibrosis in rats similar to that described for bleomycin.

Macrophages are the predominate type of immune cell in lung tissue with mast cells, lymphocytes, and dendritic cells being less prevalent. Of special importance in fibrosis are mast cells that, besides having an immune function, have recently been identified to play an important role in disease processes. Divoux *et al*., (2012) reported that mast cells were activated in human adipose tissue and were localised at regions where fibrosis occurs. Mast cells are also implicated in the development of lung fibrosis in that 5-HT is taken up from the serum via the 5-HT transporter (SERT) and carried to the site of injury where it is released. From the evaluation of the presence of mast cells shown in Figure 2 A, B and C, it is clearly seen that there is an increase in the number of mast cells in the HED and HED-S groups compared to the control group where only a few mast cells were found scattered in the lung parenchyma.

Apart from the inflammatory role of mast cells, these cells have been reported to have bidirectional effects on matrix turnover either promoting tissue repair or fibrogenesis. Cha *et al*., (2012) reported a higher mast cell density in patients with idiopathic pulmonary fibrosis (IPF) than other lung diseases such as chronic hypersensitive pneumonitis, systemic sclerosis related interstitial lung disease and normal lungs. It was also found by previous researchers that mast cell numbers are increased in drug-induced lung fibrosis (Chyczewski *et al*., 1997; Cha *et al*., 2012) Indications are that Sibutramine induces an inflammatory effect as well as regenerative fibrogenesis causing excessive collagen deposition and altered lung structure.

Lymphocytes, predominantly T cells are usually found as single cells throughout the conducting pathway of the lungs. Greater lymphoid numbers are present in lymphoid aggregates, the BALT, in the lamina propria and submucosa. These lymphoid aggregates are usually associated with areas of acute or chronic injury (Fraser, 2005; Stevens and Lowe, 2005; Pabst and Tschernig, 2010) and are known as inducible BALT (iBALT) (Rangel-Moreno *et al*., 2006). Bleomycin induced lung fibrosis, is associated with increased iBALT. Chen *et al*., (2001) reported that bleomycin induces both inflammation and fibrosis and this effect is potentiated by locally produced interferon (IFN)-δ. IFN-δ deficient mice present with significantly lower parenchymal inflammation and total hydroxyproline content. In this study increased iBALT was observed in animals fed a HED and may be related to the inflammatory profile of obesity. In addition, the HED-S group showed well defined regions of iBALT present in the terminal bronchiole. iBALT is absent in human, but in a rat model is a structural marker of inflammation and fibrosis.

This study clearly shows that Sibutramine induces fibrosis and is a function of mast cell transport of 5-HT and activation of fibrogenesis leading to increased collagen deposition and iBALT formation. An important consideration is whether this effect is permanent or reversible. No literature could be found where lung fibrosis is a side effect of Sibutramine usage. Nevertheless continual usage of Sibutramine or herbal products that contained hidden Sibutramine could lead to the development of lung fibrosis. Whether Sibutramine induced lung fibrosis is reversible following cessation of usage, as for methysergide, (Mann and Oakley, 2013) remains unknown. This aspect will be the focus of further research.

5. Conclusion

It is clear from the results obtained in this study that Sibutramine induces lung fibrosis in Sprague-Dawley rats indicated by increased collagen synthesis, mast cell accumulation and

induction of iBALT in the terminal bronchiole as well as increased collagen deposition in the respiratory tissue.

6. Acknowledgements

The authors wish to acknowledge the National Research Foundation (NRF) for funding this project as well as the Unit for Microscopy and Microanalysis at the University of Pretoria for the use of the light and transmission electron microscopes as well as Miss S Arbi for the staining of the light microscopy samples used in this manuscript.

7. References

Blaauboer, ME., Boeijen, FR., Emson, CL. 2014. Extracellular matrix proteins: A positive feedback loop in lung fibrosis? Matrix Biol, 34, 170–178

Cha, S., Chang, CS., Kim, EK et al. 2012. Lung mast cell density defines a subpopulation of patients with idiopathic pulmonary fibrosis. Histopathol. 61, 98-106.

Chen, ES., Greenlee, BM., Wills-Karp, M et al. 2001. Bleomycin-induced pulmonary fibrosis is attenuated in Interferon- γ Knockout mice. Chest. 120, 8.

Chyczewski, L., Debek, W., Chyczewska, E et al. 1997. Morphology of lung mast cells in rats treated with bleomycin. Exp. Toxicol. Pathol. 49, 409-424.

Dees C, Akhmetshina A, Zerr P et al. 2011. Platelet-derived 5-HT links vascular disease and tissue fibrosis. J. Exp. Med. 5, 961-972.

Divoux, A., Moutel, S., Poitou, C et al. 2012. Mast cell in human adipose tissue: Link with morbid obesity, inflammatory status, and diabetes. J. Clin. Endocrinol. Metab. 97(9), 1677-1685.

Eroglu, E., Gemici, G., Bayrak F et al. 2009. Acute myocardial infarction in a 24 year-old man possibly associated with sibutramine use. Int. J. Cardiol. 137, 43-45.

Fabre, A., Marchal-Somme, J., Marchand-Adam, S et al. 2008. Modulation of bleomycin-induced lung fibrosis by 5-HT receptor antagonists in mice. Eur. Respir. J. 32, 426-436.

Fraser, RS. Histology and gross anatomy of the respiratory tract, in: Hamid Q, Shannon J, Martin,J (Eds). Physiologic basis of respiratory disease. Canada. BC Decker Inc. 2005

Hwang IC, Park JY, Ahn HY, Kim KK, Suh HS, Ko KD, Kim K. 2014. Effects of CYP3A5, CYP2C19, and CYP2B6 on the clinical efficacy and adverse outcomes of sibutramine therapy: A crucial role for the CYP2B6*6 allele. Clin. Chim Acta 428, 77–81.

Izbicki, G., Segel, MJ., Christensen, TG et al. 2002. Time course of bleomycin-induced lung fibrosis. Int. J. Exp.Pathol. 83, 111-119.

Jackson, HC., Bearham, MC., Hutchins, LJ et al. 1997. Investigating the mechanisms underlying the hypophagic effects of the 5-HT and noradrenaline reuptake inhibitor, sibutramine, in the rat. Br. J. Pharmacol. 121, 1613-1618.

Latta, VD., Cecchettini, A., Del Ry, S., Morales, M.A. 2015. Bleomycin in the setting of lung fibrosis induction: from biological mechanisms to counteractions. Pharmacol Res. http://dx.doi.org/10.1016/j.phrs.2015.04.012

Lechin, F., Van Der Dijs, B., Hernandez, G et al. 2006. Neurochemical, neuroautonomic and neuropharmacological acute effects of sibutramine in healthy subjects. Neurotoxicol. 27, 184–191.

Loric, S., Maroteaux, L., Kellerman, O et al. 1995. Functional 5-HT-2B receptors are expressed by teratocarcinoma-derived cell line during 5-HTergic differentiation. Mol Pharmacol. 47, 458-466.

Luque, CA., Rey, JA. 2002. The discovery and status of sibutramine as an anti-obesity drug. *Eur. J. Pharmacol.* 440, 119-128.

Mann, DA., Oakley, F. 5-HT paracrine signalling in tissue fibrosis. 2013. Biochim. Biophys. Acta. 1832, 905-910.

Marcos, E., Fadel, E., Sanches, O et al. 2004. 5-HT-induced smooth muscle hyperplasia in various forms of human pulmonary hypertension. Circ. Res. 94, 1263-1270.

Moreira, RK. Hepatic Stellate Cells and Liver Fibrosis. 2007. *Arch. Pathol. Lab. Med.* 131(11), 1728-1734.

Oberholzer, HM., Van Der Schoor, C., Bester, MJ. 2013. Rats on a high-energy diet showing no weight gain present with ultrastructural changes associated with liver fibrosis. Ultrastruct. Pathol. 37(4), 267-272

Pabst, R., Tschernig, T. Bronchus-Associated Lymphoid Tissue: An Entry Site for Antigens for Successful Mucosal Vaccinations. 2010. Am. J. Respir. Cell. Mol. Biol. 43, 137–141.

Padwal, RS., Majumdar, SR. 2007. Drug treatments for obesity: orlistat, sibutramine, and Rimonabant. Lancet. 369, 71–77.

Phan, SH. 2002. The myofibroblasts in pulmonary fibrosis. Chest. 122, 286-289.

Rangel-Moreno, J., Hartson, L., Navarro, C, et al. 2006. Inducible bronchus-associated lymphoid tissue (iBALT) in patients with pulmonary complications of rheumatoid arthritis. J. Clin. Invest. 116(2), 3183-94.

Reagan-Shaw, S., Nihal, ML., Ahmad, N. 2007. Dose translation from animal to human studies revisited. *FASEB. J.* 22, 659–66.

Sansbury, BE and Hill, BG. 2014. Regulation of obesity and insulin resistance by nitric oxide. Free Radical Bio. Med. 73, 383–399.

Sime, PJ., O'reilly, KMA. 2001. Fibrosis of the lung and other tissues: New concepts in pathogenesis and treatment. Clin. Immunol. 99, 308-319.

Stevens, A., Lowe, J. 2005. Human Histology (3rd edn)., Elsevier: Philadelphia